Shock Waves (2004)
Digital Object Identifier (DOI) 10.1007/s00193-004-0238-1

Shock Waves

Original article

Performance of a detonation driven shock tunnel

W. Zhao[1], Z.L. Jiang[2], T. Saito[1], J.M. Lin[2], H.R. Yu[2], K. Takayama[1]

[1] Shock Wave Research Center, Institute of Fluid Science, Tohoku University, 2-1-1 Katahira, Aoba-ku, Sendai 980-8577, Japan
[2] LHD, Institute of Mechanics, Chinese Academy of Sciences, Beijing, 100080, China

Received 13 December 2003 / Accepted 26 August 2004
Published online 26 November 2004 – © Springer-Verlag 2004
Communicated by K. Takayama

Abstract. A detonation driven shock tunnel is useful as a ground test facility for hypersonic flow research. By attaching a convergent section ahead of the primary diaphragm in the driver section, the downstream operation mode became available to generate a high-enthalpy test flow. A 100 mm diameter shock tunnel was for the first time installed in the Laboratory of High-Temperature-Gas Dynamics (LHD), Institute of Mechanics, Chinese Academy of Sciences, and after its continuous refitments, a high performance detonation driven shock tunnel was achieved to generate high-enthalpy and high-Reynolds number test flows. A new method to burst a metal diaphragm with the downstream operation mode is discussed.

Key words: detonation driven, shock tunnel, shock wave, expansion waves

1 Introduction

Ground test facilities are necessary in hypersonic flow research, especially for simulating space vehicles' atmospheric reentry and supersonic combustion. Although ballistic ranges and wind tunnels with electrical arc heaters are already used for this purpose, impulse wind tunnels have advantages because these facilities can accommodate relatively large-size models and their operational costs are relatively low. Among the impulse facilities, such as free piston shock tunnels, detonation driven shock tunnels, and light-gas gun shock tunnels, the detonation driven shock tunnels were already chosen by some laboratories in the world because the detonation driven systems are inexpensive, have simple structures and a higher degree of repeatability than free piston shock tunnels.

Detonation product gases at high temperatures and pressures can easily generate strong incident shock waves in shock tubes. Two detonation driven systems are possible basically depending on the difference in ignition positions in the driver section: the system in which the ignition is performed at the end of driver section is named downstream operation mode; another system in which it is done near the primary diaphragm section is named upstream operation mode. Both of these operation modes were for the first time investigated by Bird [2]. Their elementary characteristics were analyzed. Coates and Gaydon [3] tried a double driver system, in which weak incident shock waves were generated firstly in the detonation chamber, and then the detonation was initiated by the shock wave reflected from the primary diaphragm section as shown in Fig. 1a. The detonation was not easily initiated by the reflected shock waves, and then the reproducibility was not satisfactory.

Yu et al. [8] developed a detonation driven shock tunnel, in which, as shown in Fig. 2, a damping section was connected to the end of the driver section and the igniter was placed near the primary diaphragm section.

Based on this idea, a series of detonation driven shock tunnel facilities were successively constructed at LHD, Institute of Mechanics, Chinese Academy of Sciences and the Shock Waves Laboratory, RWTH Aachen University [5].

Bakos and Erdos [1] developed double driver sections. To simultaneously ignite oxy-hydrogen mixtures, high-pressure helium is filled in the first driver section as shown in Fig. 1b. The detonation driver was applied in both reflected shock tunnel and expansion tunnel, and high-enthalpy tests were carried out on this facility.

The downstream and upstream modes were studied at LHD [9] and crucial techniques, such as spontaneous strong ignition and attenuation of the reflected waves, were resolved successively. As a result of these improvements, a large detonation driven shock tunnel was constructed in 1996, which was 40 m in total length, had a

Correspondence to: W.Zhao
(e-mail:wzhao@rainbow.ifs.tohoku.ac.jp)

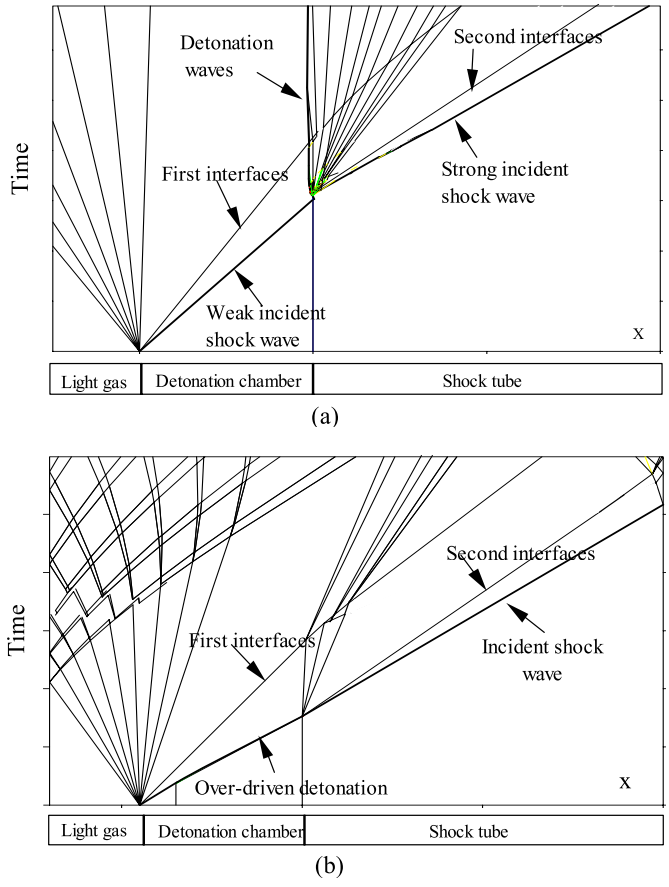

Fig. 1a,b. x-t wave diagram of detonation driven shock tube with two kinds of ignition, **a** Initiation by the reflection of a shock wave, **b** Initiation by a strong incident shock wave

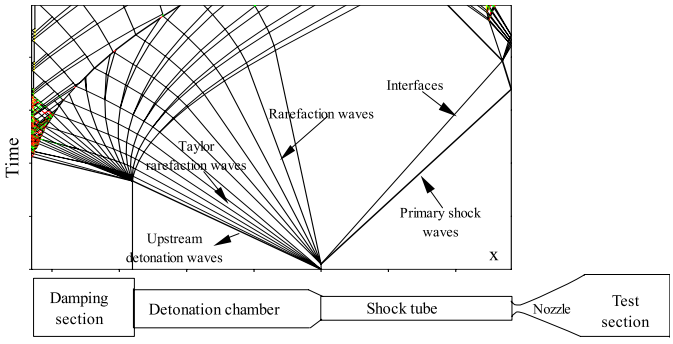

Fig. 2. x-t wave diagram of upstream operation mode

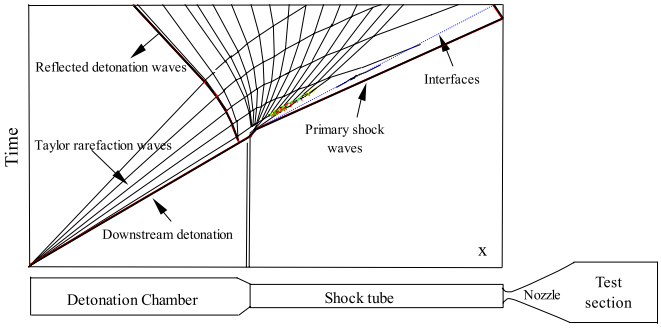

Fig. 3. x-t wave diagram of downstream mode detonation driven shock tube with with a convergence section

conical nozzle with 500 mm in exit diameter, and was operated at an operational pressure in the detonation chamber of 300 MPa.

The downstream operation mode is advantageous for obtaining high-enthalpy test flows. However, due to the Taylor rarefaction wave which follows the detonation front, the primary shock wave is attenuated. Jiang et al. [7] and Zhao et al. [10] developed some ways to solve these problems. Another problem to solve then was to burst the primary metal diaphragms, which produced fragments at the moment of rupture. To avoid this effect, plastic diaphragms are employed in some laboratories although these also have demerits. A new method was developed in LHD to burst metal diaphragms without creating any fragments. With this technique, 25 MPa stagnation pressure and 15 MJ/kg stagnation enthalpy was achieved at an initial driver pressure of 3.5 MPa.

The upstream operation mode with the damping section is used to generate test flows with high-Reynolds numbers of over 4×10^7/m.

This paper reports the detonation driven shock tunnel's performance with upstream and downstream operation modes and the newly developed diaphragm burst technique.

2 Operation principle

2.1 Upstream operation mode

To explain the principle of the upstream operation mode accompanying a damping section, the waves propagation in the detonation driven shock tube is presented in Fig. 2 in the x-t diagram. The detonation wave is initiated near the primary diaphragm, and propagates to the reverse direction and eventually bursts the diaphragm at the damping section at low pressure. This process attenuates the shock wave propagating along the damping section so that the reflected shock wave pressure from the end wall of the damping section cannot be very high. Meanwhile, the high-temperature and high-pressure detonated product gas which remains in the driver section acts as the driver source for the shock tube. After the primary diaphragm rupture, a strong incident shock wave propagates toward the shock tube end wall. The nozzle reservoir condition is generated similarly to conventional reflected shock tunnels.

The damping section works to decrease the reflected shock pressure. Without the damping section, detonation waves reflected from the end wall of the high pressure chamber would create hundred times higher pressure of the initial pressure [4], it may damage the facility.

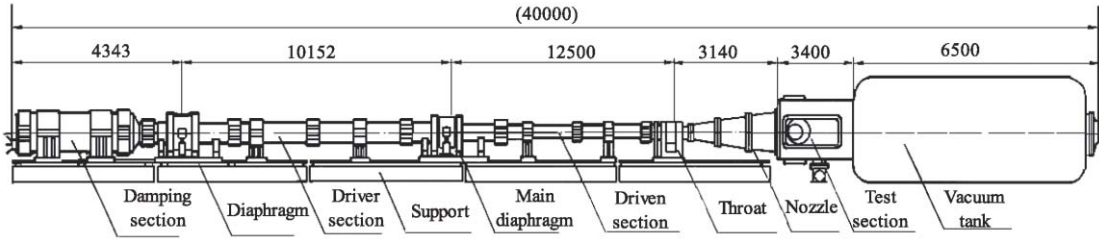

Fig. 4. Sketch of the JF-10 detonation shock tunnel

2.2 Downstream operation mode

The downstream operation mode is explained in the x-t diagram shown in Fig. 3. An area converging section is placed in front of the primary diaphragm section of the detonation chamber. The Taylor rarefaction wave which follows up the downstream propagating detonation front will be accelerated after passing the area converging section, and attenuates the primary shock wave. The area converging section gives a simple and useful method to solve the quick shock attenuation due to the Taylor rarefaction wave, because the reflected detonation wave at the area convergence will weaken the Taylor rarefaction wave. However, this method has a limitation which is only valid if the Taylor rarefaction wave is not too strong to be weakened fully. If the primary shock wave is so fast as for the rarefaction wave to catch it up, then the downstream operation mode becomes available. For this purpose, initial pressures in the detonation chamber should be high enough to generate strong incident shock waves.

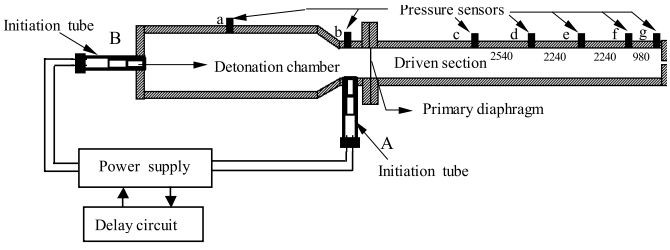

Fig. 5. Schematic illustration of the initiation tube arrangement in the downstream detonation driven shock tunnel

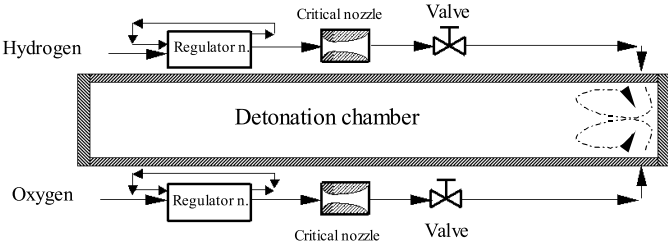

Fig. 6. Illustration of filling and mixing oxy-hydrogen with critical nozzles

3 Experimental facility

3.1 Main facility

The sketch of the JF-10 detonation tunnel is shown in Fig. 4. It is 40 m in total length, the detonation chamber has an inner diameter of 150 mm, the shock tube one of 100 mm and the damping section one of 430 mm. Under the downstream operation mode, the lengths of the detonation chamber and shock tube are 8.8 m and 12.5 m, respectively. The vacuum tank volume is nearly 25 m^3.

As the detonated product gas temperature is over 3000 K, and the flow duration is more than several milliseconds, any gaps which may exist between the detonation chamber and the diaphragm section will damage the structure. For safety, the chamber is made of PCrNi3MoVa steel, which can withstand high-pressure and high-temperature conditions. The design pressure of the detonation chamber is over 300 MPa.

3.2 Accessory facility

An initiation tube which is a shock tube consisting of an explosion wire with several convergence stages inside, was developed to quickly initiate the oxy-hydrogen mixture connected to the detonation chamber. The mixtures is ignited by the explosion wire inside the initiation tube and then a high-temperature jet is formed which propagates into the driver chamber tube, then initiates the detonation immediately as shown in Fig. 5.

In order to burst a metal diaphragm without its fragmentation under the downstream operation mode, two initiation tubes are placed near the primary diaphragm and in the end wall of the detonation chamber as shown in Fig. 5. They are not ignited simultaneously but with a delay time of several milliseconds which is set to ignite the initiation tubes of A and B. The ignition in the initiation tube A is performed just before the arrival of detonation waves at the primary diaphragm position. The delay time is specified depending on the detonation chamber length and the detonation wave speed. As the delay time is very sensitive to controlled diaphragm bursting, it should be set within 50 μs accuracy.

For the upstream operation mode, only the initiation tube A is used and the initiation tube B not. As the detonation waves propagates upstream (left), the momentum working on the primary diaphragm is less so that metal diaphragm grooves are not fragmented easily.

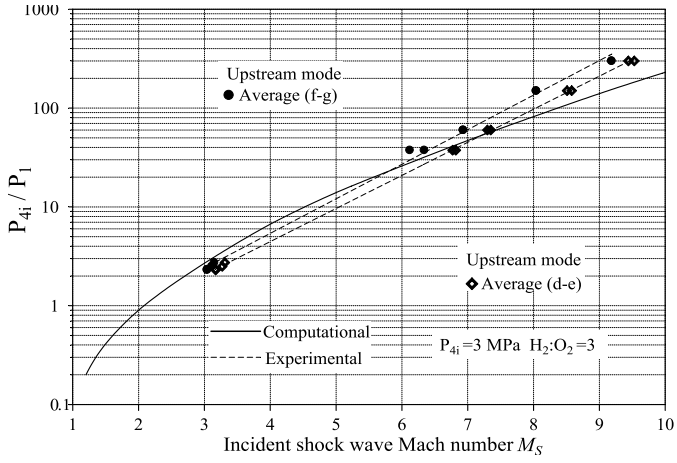

Fig. 7. P_{4i}/P_1 vs M_s under upstream operation mode

Five pressure sensors were arranged along the shock tube to detect to shock wave arrival at the positions marked (c,d,e,f,g) as seen in Fig. 5. The reservoir conditions of the shock tunnel are determined by the output signals from (f,g) installed near the throat. The pressure transducers (a,b) were installed in the detonation chamber to measure the detonation wave speed.

Oxygen and hydrogen are supplied to the detonation chamber simultaneously through critical nozzles, and mixed spontaneously by jet interaction when these gases are introduced through counter positioned outlet nozzles inside the chamber as seen in Fig. 6. Based on the critical nozzle principle, the constituents of stoichiometric oxyhydrogen mixtures were accurately calibrated.

The exit diameter of the hypersonic nozzle is 500 mm. Two types of throats are designed to correspond to Ma = 8 and Ma = 10 flow fields and the corresponding throat diameters are $d^* = 33$ mm and 16 mm, respectively. A pitot rake of 550 mm in radial length was used to measure free stream pressures in the test section. The pressure transducers were distributed at every 50 mm.

4 Experimental results and discussion

According to the definition of the conventional shock tunnel terminology, subscript "4i" and subscript "1" represent the initial condition in the detonation chamber and that in the driven section, respectively. "M_s" represents the primary shock wave Mach-Number in the shock tube, "M_a" represents the free stream Mach-Number in the test section. All of the experiments were carried out under the following conditions:

$P_{4i} = 3$ MPa$\sim$4.9 MPa, mixture $H_2 : O_2 = 2 \sim 4.5$,
$P_1 = 0.01$ MPa$\sim$2.2 MPa, Air.

4.1 Results of upstream driven detonation

The relationship between the P_{4i}/P_1 and M_s is shown in Fig. 7, where $P_{4i} = 3$ MPa and $H_2 : O_2 = 3$. The difference between the two black lines at the same P_{4i}/P_1 condition represents the shock wave attenuation from "d" to "g". Figure 7 shows that the increase of the pressure ratio with Mach Number for these two lines is small and with very limited shock wave attenuation.

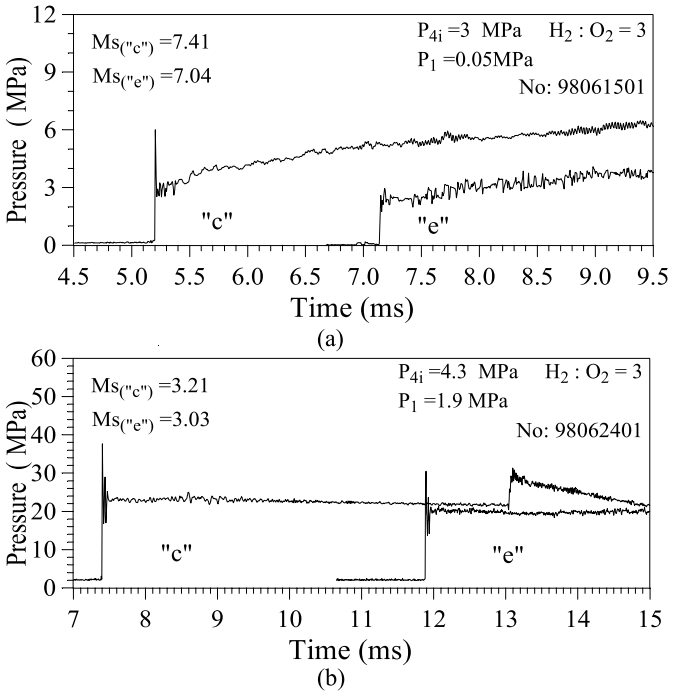

Fig. 8a,b. Typical experimental pressure histories in the shock tube under upstream operation mode

Departures between computational and experimental results should be noticed. The predicted value of P_{4i}/P_1 is higher than the experimental one when the Mach number is less than 6. This might be caused by the increase of the throat diameter from 100 mm to 150 mm in the driver section, and additional driving is generated. On the other hand, the predicted value of P_{4i}/P_1 is lower than the experimental one when the Mach number exceeds 6. This may be attributable to the existence of viscosity and heat conduction in shock tube flows. The stronger the incident shock waves, the more serious the shock wave attenuation becomes.

Figure 8 shows typical pressure histories recorded at "c" and "e": A strong shock case is shown in Fig. 8a and a moderate shock case in Fig. 8b. In the strong shock case, expansion waves are so intense that the expansion tail matches with the interface. A stable pressure plateau continues for a short time duration and increases gradually. With propagation, the pressure profile becomes flat, while the shock strength attenuates from "c" ($M_s = 7.41$) to "e" ($M_s = 7.04$). It indicates that to achieve a stable test time, the shock tube should be long despite of significant shock attenuation.

For a moderate incident shock, the effect of expansion waves is limited and then the plateau pressures continues relatively long as seen in Fig. 8b. The shock attenuated from "c" ($M_s = 3.21$) to "e" ($M_s = 3.03$).

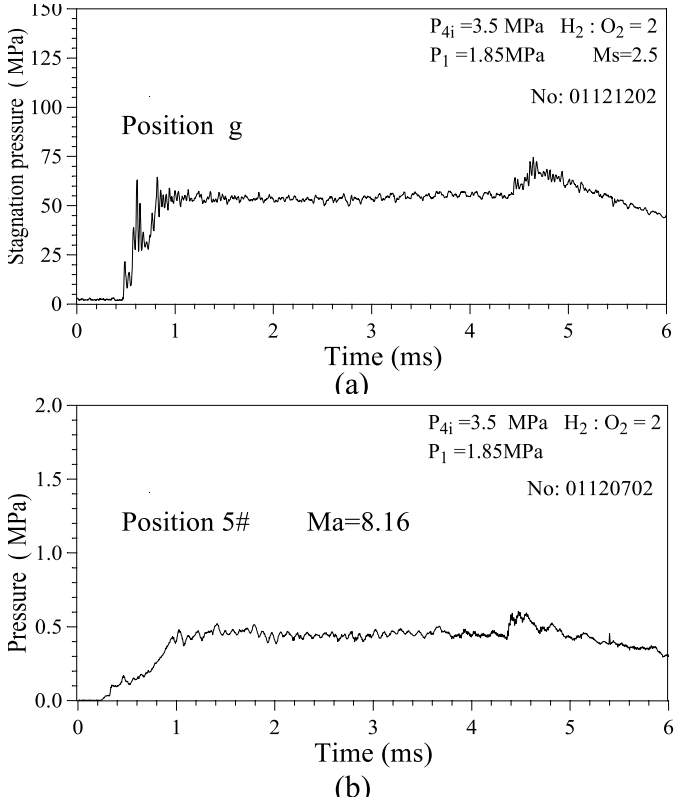

Fig. 9a,b. Pressure histories under upstream mode **a** reservoir pressure histories, **b** pitot pressure histories

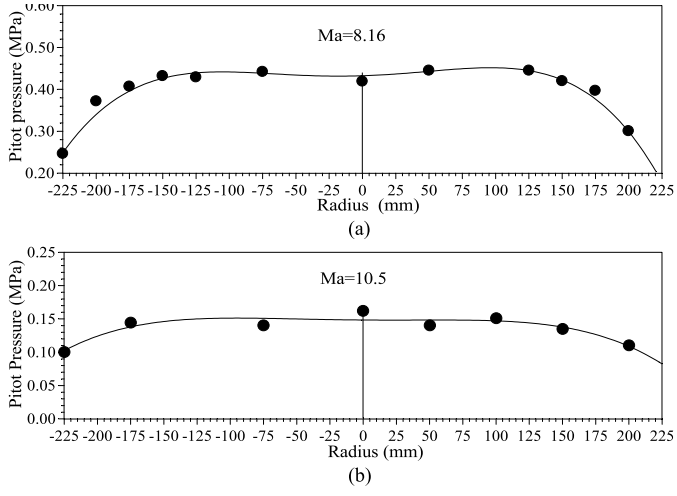

Fig. 10a,b. Pitot pressure distributions at the exit of nozzle under upstream mode

Although limited in the generation of high-enthalpy flows, the upstream operation mode could generate high Reynolds number flows because of the excellent performance at low-enthalpy conditions.

Typical stagnation pressure histories and pitot pressure histories are shown in Fig. 9. At a 27 mm distance from the transducer "g" to the second diaphragm, the pressure transducer was installed in a recess mount, which

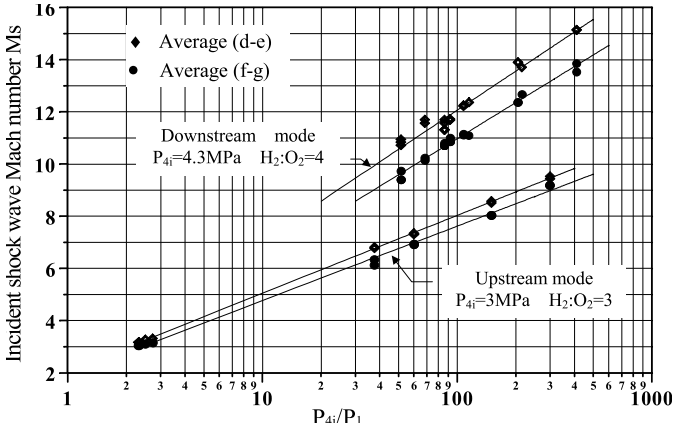

Fig. 11. M_s vs P_{4i}/P_1 under downstream operation mode and upstream mode

Table 1. Initiation conditions and free stream parameters

P_{4i}	H_2/O_2	P_0	H_0	M_a	U_∞	Re
MPa		MPa	MJ/kg		m/s	$1/m$
3.5	2	55.3	0.68	8.16	1380	4×10^7
3.5	2.5	60.2	1.06	10.5	1430	2×10^7

caused a spike-shaped pressure history at the earlier stage as seen in Fig. 9a and gradual pressure increase behind the shock jump as seen in Fig. 9b, which is attributable to the arrangement of protecting the pressure transducers from high temperature test flow by filling a 6 mm thick silicone gel in the recess mount cavity. However, the steady reservoir condition continues for about 3.5 ms.

Two low-enthalpy conditions were tested, the initial conditions and free stream parameters of which are presented in Table 1. The free stream speed U_∞ is limited but the Reynolds numbers are kept high.

Pitot pressure distributions across the nozzle exit are shown in Fig. 10: in the case of $M_a = 8.16$ in Fig. 10a; $M_a = 10.5$ in Fig. 10b with the throat diameters of 33 mm and 16 mm, respectively.

4.2 Results of downstream operation mode

Due to the Taylor rarefaction waves and viscosity and heat conduction along the shock tube wall, the primary shock wave attenuates from the beginning of propagation. Figure 11 shows the relationship between M_s and P_{4i}/P_1 for both downstream mode and upstream mode. Comparing the result of upstream mode with downstream mode, even though we can see significant shock attenuation in the downstream mode, the P_{4i}/P_1 which creates the identical M_s value is only 10% of that in the case of upstream operation mode, especially for high M_s values. For example, at identical $M_s \approx 9$, the $P_{4i}/P_1 \approx 30$, but in the upstream mode $P_{4i}/P_1 \approx 300$.

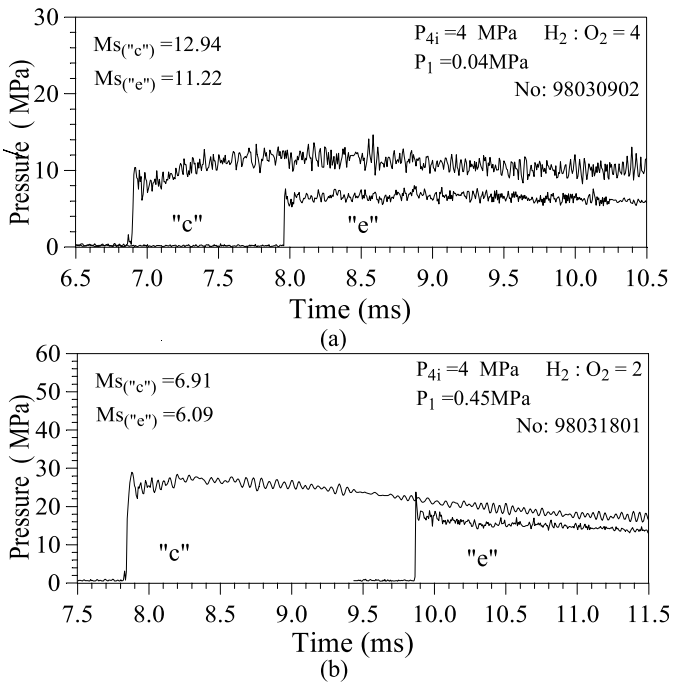

Fig. 12a,b. Typical experimental pressure histories in the shock tube under downstream operation mode

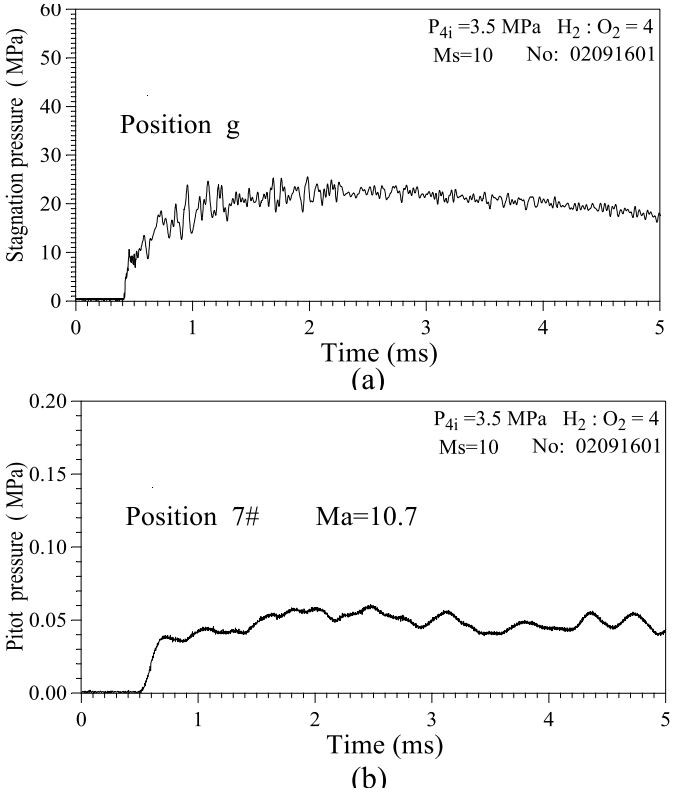

Fig. 13a,b. Pressure histories under downstream mode **a** reservoir pressure histories, **b** pitot pressure histories

The attenuation mechanism is different depending on P_{4i}/P_1 values. For P_{4i}/P_1 lower than 50, the incident shock attenuation is caused mainly by the overtaking of rarefication waves. For P_{4i}/P_1 higher than 50, the shock attenuation is attributable to the effect of viscosity and heat conduction, and the region behind shock waves becomes stable after a certain propagation distance.

Typical pressure histories in the shock tube in downstream operation mode are shown in Fig. 12: for P_{4i}/P_1 = 100 in Fig. 12a; and $P_{4i}/P_1 \doteq 9$ in Fig. 12b.

In Fig. 12a for a strong shock, the arrival of the rarefaction wave is delayed. At the earlier stage, the expansion tail matches with the interface, the pressure behind the shock wave increases slightly as seen in "*c*" in Fig. 12a. With propagation, the pressure behind the shock wave becomes uniform as seen in "*e*" in Fig. 12a, whereas the Mach number decreases from 12.94 to 11.22.

Balanced by the expansion tail and the Taylor rarefaction wave, the plateau post-shock pressure appears at first, then decreases gradually as seen in "*c*" in Fig. 12b. The incident shock overtaken by the Taylor rarefaction wave is attenuated with propagation as seen in "*e*" in Fig. 12b.

Typical stagnation pressure and pitot pressure histories obtained in the downstream operation mode are shown in Fig. 13, in which the test condition is overtailored, and the initial condition and free stream parameters are shown in Table 2.

The data deduction carried out only by pitot pressure measurements is not enough to validate the real flow condition, other measures such as heat-flux measurements and spectrum analysis are necessary to fully detect the flow characteristics, which were already reported in [7].

Table 2. Initiation conditions and free stream parameters

P_{4i}	H_2/O_2	P_0	H_0	M_a	U_∞	Re
MPa		MPa	MJ/kg		m/s	1/m
3.5	4	22.1	14.3	10.7	4860	1.7×10^7

The amount of transducers consumed during the test is high, few are working normally at last. However, the pitot pressure distribution across the nozzle exit is shown in Fig. 14. The uniform nozzle flow diameter is nearly 350 mm.

A new method for bursting metal diaphragms is to ignite two initiation tubes separately in a time controlled fashion, in which a delay circuit is used. As the electrical current needed for igniting the explosion wire is intense, a problem focuses on the calibration of the interval precision within 50 μs. The broken diaphragms are shown in Fig. 15, which clearly shows no fragments produced during their rupture.

5 Conclusion and perspectives

The detonation driven shock tunnel was installed at LHD, in which both the downstream operation mode and the upstream operation mode were examined to generate high-

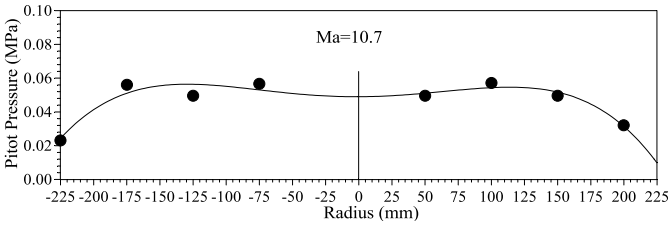

Fig. 14. Pitot pressure distribution at the exit of nozzle under upstream mode

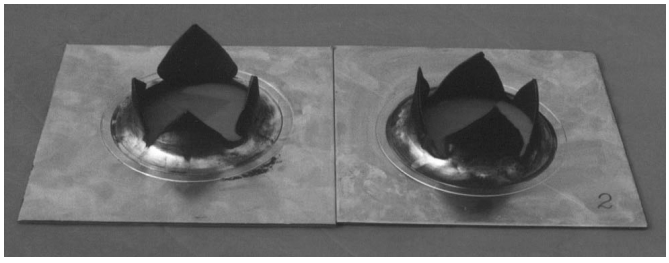

Fig. 15. Broken diaphragms with two initiation tubes

enthalpy flows. The former was ten times stronger than that of the latter in driving power to generate the high-enthalpy test flow, also the primary shock wave attenuation is little serious but on sufferance.

For the downstream mode operation, due to the Taylor rarefaction waves, the primary shock wave decays seriously when P_{4i}/P_1 is low. But when the P_{4i}/P_1 value exceeding 50 with the convergent section connected near the primary diaphragm, high-enthalpy test flows were generated. The high-enthalpy condition with 22 MPa stagnation pressure and 14 MJ/kg stagnation enthalpy was obtained, which also generated a 4.8 km/s free stream and a test time of about 3.5 ms. The detonation driven shock tunnel performance would be improved significantly by increasing the initial pressure P_{4i} and keeping high P_{4i}/P_1.

The upstream detonation driven shock tunnel is advantageous for generating low enthalpy test flows. At 3.5 MPa initial pressure in oxy-hydrogen mixture, the reservoir pressure of more than 60 MPa was obtained, and the flow field was relatively uniform.

By using a specially designed delay circuit, a new method to break the diaphragm was developed, whose performance was validated in the downstream detonation driven shock tunnel.

It is concluded that the detonation driven shock tunnel can be a useful ground test facility for the simulation of hypersonic flights at either a high-enthalpy condition or a high-Reynolds number.

References

1. Bakos, R.J., Erdos, J.I.: Optimizing pressure recovery in a detonation driven reflected shock tunnel. In: Houwing, A.F.P., Paull, A. (eds.) Shock Waves. Panther Publishing and Printing, Canberra, Australia, 1997, pp. 1359–1365
2. Bird, G.A.: A note on combustion driven tubes. Royal Aircraft Establishment, AGARD Rep. 146, B-VII, 1957
3. Coates, P.B., Gaydon, A.G.: A simple shock tube with detonating driver gas. Proc. Roy. Soc. (London) A **283**, 18–32 (1964)
4. Edwards, D.H., Williams, G.T., Breeze, J.C.: Pressure and velocity measurements on detonation waves in hydrogen-oxygen mixtures. J. Fluid Mech. **6**, 497–517 (1959)
5. Grönig, H., Olivier, H., Habermann, M.: Development of a detonation driver for a shock tunnel. A Review. High Pressure Science Technology **7**, 879–884 (1997)
6. Jiang, Z.L., Zhao, W., Lin, Z.B.: Progresses in the detonation driven shock tunnel and the moment measurement technique. J Advances in Mech (in Chinese) **31**, 312–317 (2001)
7. Jiang, Z.L., Zhao, W., Wang, C., Takayama, K.: Forward-running detonation drivers for high-enthalpy shock tunnels. AIAA J **40**, 2009–2016 (2002)
8. Yu, H.R., Esser, B., Lenartz, M., Grönig, H.: Gaseous detonation driver for a shock tunnel. Shock Waves 2: 245–254 (1992)
9. Yu, H.R., Zhao, W.: The use of oxy-hydrogen detonation driver for generation of high enthalpy flow. In: Proc. 20th International Symposium on Rarefied Gasdynamics, Beijing, China, 1997, pp. 927–933
10. Zhao, W., Wang, C., Jiang, Z.L.: Research on forward running detonation drivers for generation of high-enthalpy flows. In Proc First Internal Symposium on Advanced Fluid Inf, Sendai, Japan, 2001, pp. 521–523